Technology and Innovation, Vol. 21, pp. 1-20, 2020
Printed in the USA. All rights reserved.

ISSN 1949-8241 • E-ISSN 1949-825X
http://dx.doi.org/10.21300/21.4.2020.9
www.technologyandinnovation.org

COLLAGEN-PEPTIDE-BASED DRUG DELIVERY STRATEGIES

Arthi Jayaraman[1,2], Christopher Price[3], Millicent O. Sullivan[1,3], and Kristi L. Kiick[2,3,4]

1. Department of Chemical and Biomolecular Engineering, University of Delaware, Newark, DE, USA
2. Department of Materials Science and Engineering, University of Delaware, Newark, DE, USA
3. Department of Biomedical Engineering, University of Delaware, Newark, DE, USA
4. Delaware Biotechnology Institute, Newark, DE, USA

Collagen-targeting strategies have proven to be an effective method for targeting drugs to pathological tissues for treatment of disease. The use of collagen-like peptides for controlling the assembly of drug delivery vehicles, as well as their integration into collagen-containing matrices, offers significant advantages for tuning the morphologies of assembled structures, their thermoresponsiveness, and the loading and release of both small-molecule and macromolecular cargo. In this contribution, we summarize the design and development of collagen-peptide-based drug delivery systems introduced by the Kiick group and detail the expansion of our understanding and the application of these unique molecules through collaborations with experts in computational simulations (Jayaraman), osteoarthritis (Price), and gene delivery (Sullivan). Kiick was inducted as a Fellow of the National Academy of Inventors in 2019 and was to deliver an address describing the innovations of her research. Given the cancellation of the NAI Annual Meeting as a result of coronavirus travel restrictions, her work based on collagen-peptide-mediated assembly is instead summarized in this contribution.

Key words: Collagen peptides; Drug delivery; Extracellular matrix; Osteoarthritis; Wound healing

INTRODUCTION

The Extracellular Matrix and Collagen

An expanded understanding of the interactions between cells and the extracellular matrix (ECM), as well as increased knowledge about signaling pathways and molecules relevant to the treatment of disease, has been applied over the past decade in designing cell-specific therapeutics and drug delivery systems (1-5). Given collagen's role as the major ECM component—providing mechanical support, regulating cellular behaviour, and directing tissue development—many of these studies have explored means to capture the physical properties and/or the biological signalling properties of the matrix via the

Accepted: September 1, 2020.
Address correspondence to Kristi L. Kiick, FNAI, University of Delaware, 201 DuPont Hall, Newark, DE 19716, USA. Tel: +1-302-831-0201. Email: kiick@udel.edu

use of polymers, biopolymers, and peptides. One key structural feature of collagen—its formation of triple-helical fibrils—has offered many strategies in the design of therapeutics. In addition, collagen's integrin-mediated interactions with cells to regulate adhesion, proliferation, and migration provide additional handles for tuning bioactivity.

Collagen is widely used as a natural material for biomedical application and as a matrix for drug delivery (6-9), controlling the delivery of drugs such as small molecules, proteins, and genes via simple diffusion and/or biodegradation. Collagen matrices have been loaded with a variety of small molecules, such as antibiotics for wound care, cisplatin for local cancer therapy, and anti-inflammatory reagents for tissue regeneration in ophthalmology (10). Small molecule gentamicin-eluting collagen matrix Collatamp® (Schering-Plough, Stockholm, Sweden), Sulmycin®-Implant (Schering-Plough, USA), and Septocoll® (Biomet, Merck, Germany) have been used in the clinic as wound care products to promote both granulation tissue formation and epithelialization as well as to protect tissues from potential infection (11).

In addition to direct encapsulation of molecules into collagen-based matrices, molecules modified with collagen-binding domains (CBDs) also have been attached to drugs or polymeric carriers to enable their immobilization in collagen-based hydrogel matrices for sustained drug release. Studies with CBDs derived from collagenase or fibronectin have been employed to tether the synthetic human antimicrobial peptide cathelicidin LL37 on collagen scaffolds for treatment of wound infections (12). Similar strategies using CBDs have been employed for the targeting and release of both immune checkpoint inhibitor antibodies (αCTLA4 + αPD-L1) and interleukin-2 (IL-2) using CBDs derived from von Willebrand factor for cancer immunotherapy (13). Overall, these examples demonstrate that the peptide-based immobilization of therapeutic agents in collagen-containing hydrogels can prolong their effectiveness via controlled release from the scaffold and suggests the utility and promise of the approach.

A wide variety of collagen-peptide-based materials have therefore been developed, with aims of understanding the mechanisms by which collagen fibrils form in vivo and for developing nanoscale fibrils, nanostructures, and hydrogel materials. Many studies have demonstrated that unfolded collagen-like peptides (CLPs) can target native collagens or collagen substrates via the formation of triple helix (14,15) and that short CLPs can be used to form and modify hydrogels, liposomes, and other structures (16-18). Despite their prevalence in these types of investigations, however, they have not been used as a design element to affect nanoparticle assembly via manipulation of lower critical solution temperature (LCST) transitions. Such application of CLPs, which is the focus of our group's work, should be very fruitful given their hydrophilicity, rod-like triple-helical structure, and ability to integrate in collagen-containing matrices. The approaches should also be valuable for producing nanostructures that can target the collagen in pathological connective tissue.

ECM-based Pathologies: Osteoarthritis

There are multiple pathological conditions characterized by aberrant remodeling of the ECM (and collagen), including cancers of organs and tissues, deficiencies in development of skeletal tissue, arthroses, and chronic wounds. We have been investigating the opportunities for collagen-peptide-modified delivery vehicles for the latter two of these applications, with an aim toward developing collagen-targeting carriers that can deliver small-molecule and macromolecular cargo. Osteoarthritis (OA) is the most common form of arthritis (19), affecting nearly 23 million people in the United States (20) and 240 million people worldwide (21), with these numbers expected to increase as the population ages (22). The hallmark indicators of OA are inflammation, remodeling, and degradation of the cartilage ECM, leading to the loss of proteoglycans and collagen II (23-29). Intra-articular injection of therapeutics to the affected joint has remained a primary treatment of OA (30), allowing for the delivery of small-molecule and macromolecular drugs to address local inflammation and pain; for example, the IA injection of the corticosteroid dexamethasone is used to periodically alleviate inflammation and pain and provide some disease-modifying activity (31).

However, the extremely rapid clearance of molecules, both small and large, from the joint space significantly limits their residence times and efficacy, and thus typically necessitates injections of very high

doses. Indeed, the half-lives of drugs administered to the synovium have been reported to be on the order of tens of minutes to a few hours (32-34), and their efficacy remains equivocal (32,35-40). Furthermore, there is reluctance to perform more than two to four intra-articular (IA) injections to the joint per year owing to the risk of infection accompanying each injection and counterindications of potential chondrotoxicity due to very high local drug concentrations (32,41,42). Methods to retain drugs at the joint after IA injection would enable significantly lower doses to be administered, thus avoiding these complications.

A variety of hydrogel and nano-/micro-particulate vehicles based on polymeric materials and self-assembled small molecules have thus been explored for IA delivery of therapeutics. Several studies utilizing biodegradable polymeric microparticles have demonstrated increased physical retention in the joint (from hours to weeks) owing to limitation in diffusion and phagocytosis because of the relatively large size of the particles (> 5μm). The use of cationic nanocarriers instead allows for electrostatic retention within the anionic proteoglycan-rich cartilage, thus allowing not only retention but also penetration of the carriers into the dense ECM (43,44). Although the delivery of small molecules has been aimed largely at the alleviation of inflammation, longer-term sequestration and tissue penetration, especially of drugs such as glucocorticoids, should improve therapeutic outcomes and promote disease-modifying effects (45).

Collagen-targeting approaches have significant potential advantages in IA administration and CLPs have been widely demonstrated to hybridize/bind to denatured and degraded collagen (46-50) through triple-helical folding of a single monomeric strand of CLP with denatured collagen protein chains (51). CLPs and type-II collagen-binding peptides have been demonstrated to target collagen in healthy cartilage (52), an effect which should be enhanced by the binding to the denatured and degraded collagen II characteristic of OA cartilage. Opportunities are promising for nanocarriers that not only can bind to collagen and sequester drugs but that also can modify release profiles with external stimuli, such as modest changes in temperature.

ECM-based Pathologies: Chronic Wounds

Like the large impact of arthroses, chronic non-healing wounds have enormous health and economic impacts, occurring at a prevalence of 1% to 2% within the general population of developed countries and with total estimated costs in excess of $20 billion annually (53). Chronic wounds result from irregularities in the cellular processes that are normally coordinated in the healing of wounds, which involve a synchronized suite of activities by macrophages, fibroblasts, keratinocytes, and endothelial cells, among other cell types (54,55).

The orchestration of these cellular activities is governed by a number of growth factors (GF), and many studies and clinical trials have examined the efficacy of topical and sustained release of GF formulations in chronic wounds. Indeed, a topical platelet-derived growth factor-BB (PDBF-BB) gel was, over 20 years ago, the first successful GF treatment approved by the U.S. Food and Drug Administration (FDA) for the treatment of diabetic foot ulcers (DFUs) (56). Although these therapies provide benefit, the FDA concluded, based on clinical trial data, that topically-applied PDGF-BB increased the number of healed DFU patients by less than 10% (57). Clinical failure has been attributed to incompatibilities of traditional GF therapies with the inflammatory environment of the chronic wound, which causes significant degradation of GF. High dosing is thus required, which can lead to undesirable side effects stemming from high local and/or systemic levels following topical administration (58). In addition, the complexity of the wound healing process requires the cell-coordinated activity of specific GFs (59), suggesting that cell-mediated strategies to enhance delivery would be of significant value.

The delivery of genes that encode transient expression of desired GFs by endogenous cells has thus remained of interest for these localized applications. GF gene therapies offer exciting potential for improved GF delivery due to their ability to foster localized, cell-mediated GF production within the wound bed. GF gene delivery also offers practical advantages, including minimization of adverse effects (which include increased cancer risk or ectopic tissue formation from systemic exposure) (60) and reduction of cost as compared to topical delivery

of recombinant GF (50). Moreover, GF gene delivery has shown improved therapeutic effects with orders-of-magnitude (≈ 2000-fold) dose reductions compared to topically administered GFs (49). While clinical data on GF gene therapies are limited, localized gene therapy approaches show promise for improved safety and efficacy and are amongst the most rapidly advancing gene therapies in clinical trials for diseases such as ocular disorders and ischemic diseases (61).

Scaffold-mediated gene transfer is a particularly appealing topical treatment option due to its capacity to increase the stability of gene cargoes and provide cell-mediated control over gene production in situ within the healing site (62,63). Collagen scaffolds represent an especially interesting option because of the wide usage of collagen in the treatment of chronic wounds (64). Artificial skins, such as Regranex® (Smith & Nephew), Apligraf® (Organogenesis), and Dermagraft® (Advanced Biohealing), have been shown to enhance chronic wound repair even in the absence of incorporated GFs; however, the incidence of complete closure after a therapeutic trial with engineered skin remained only ~50%, highlighting the need for improved bioactivity (65). The immobilization of DNA onto collagen-based scaffolds can improve retention (by ca. 30%) and increase gene transfection (by ca. 2-fold) (66-71), which could augment the therapeutic potential of collagen-comprising matrices.

Our research efforts with collagen-peptide-modified drug carriers have thus been broadly aimed at designing carriers that can carry small-molecule (for OA) or macromolecular cargo (for wound healing) to affected tissues. We have exploited features of two of the key structural proteins in mammals—collagen and elastin—and developed interdisciplinary teams to understand peptide assembly, formation of select nanostructures, and effectiveness at loading drugs and targeting delivery from collagen-containing matrices.

DEVELOPMENT OF CLP-BASED THERAPEUTIC NANOSTRUCTURES

CLP-modified Self-assembling Conjugates

The self-assembly of peptides has remained an active area of research for decades given the benefits

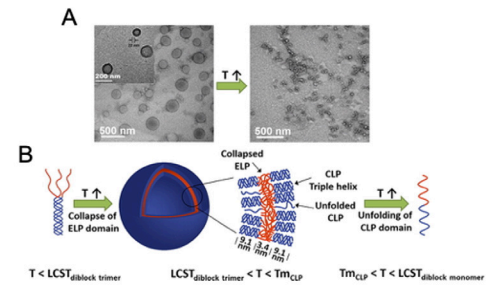

Figure 1. ELP-CLP vesicles assembly/disassembly (139). (A) TEM images of nanoparticles of the ELP-CLP conjugates. (B) Proposed scheme for ELP-CLP nanovesicles and its bilayer structure. Reprinted with permission from the American Chemical Society, copyright 2015.

of converging concepts in biology and materials science to develop functional materials (72,73). The information encoded in amino acid sequences controls chain conformations, local interactions, and hierarchical assembly with great fidelity. The significantly expanded chemical functionality of peptides offers new materials that can act not only as sensors, delivery vehicles, catalysts, and energy-harnessing structures but also as mediators and models of cell behavior (74-79). While peptides lack the ternary structures of longer proteins, the utilization of well-defined α-helical, triple-helical, β-sheet, and coiled-coil peptides has resulted in an enormous number of assembled structures (80-84). Essentially all studies have relied on peptides that adopt defined secondary structures in order to trigger assembly (e.g., with pH, ionic strength, ligand binding), largely into micellar, fibrillar/tubular, and sheet-like structures.

Because of the practical advantages for developing collagen-containing matrices, there has been an enormous body of work on developing collagen-based peptides to understand the assembly of natural collagen and to generate synthetic matrices that retain some of the assembly and biological activities of collagen, while adding chemical and synthetic versatility to their design (85). A typical CLP possesses a $(Glycine\text{-}X\text{-}Y)_n$ repeat sequence where n is between 6 and 10 repeats and the X and Y residues are usually proline (P) and hydroxyproline (O), respectively (86,87). CLPs can fold reversibly into

triple-helical secondary structures, and the midpoint of this transition is known as the melting temperature (T_m) (86,87). Short synthetic CLPs have been widely studied to understand the stabilization of specific peptide sequences in collagen triple helices (88-93), to understand the thermoresponsiveness of the collagen conformational transitions (89,94-97), and to mimic collagen fibril formation (96,98-100). Many studies have demonstrated that unfolded CLPs can target native collagens or collagen substrates via triple helix formation/invasion (15,46,101) and that short CLPs can be used to form and modify hydrogels, make nanoparticles, and generate other assemblies (16,18,102-104). In spite of such applications, the use of CLPs as building blocks in assembled nanostructures for drug delivery has been less frequently reported (16,104-106).

Table 1. Identity and Properties of Select ELP-CLP Conjugates

ELP*	CLP	T_t < vesicles < T_m **		Diameter ***
F6	$(GPO)_3GFOGER(GPO)_3$	20°C	35°C	50 nm (at 25°C)
F6	$(GPO)_7$	15°C	50°C	95 nm
F6	$(GPO)_8$	20°C	58°C	100 nm
F6	$(GPP)_{10}$	TBD	60°C	60 nm
F5Y	$(GPO)_8$	20°C	58°C	140 nm
F4Y2	$(GPO)_8$	17°C	57°C	250 nm
F5	$(GPO)_8$	33°C	56°C	200 nm
W2F2	$(GPO)_6$	15°C	40°C	250 nm

* ELP sequences denoted by the identity of the X residue in a $(VPGXG)_6$ peptide; e.g., F4Y2 denotes a sequence with the four N-terminal VPGFG and two C-terminal VPGYG repeats.

** T_t and T_m values determined by, respectively, first derivative fits of turbidity vs. temperature in DLS and of mean residue ellipticity at 225 nm vs. temperature in CD measurements, either in water (or PBS for F6-GFOGER). Repeated measurements yield measured transition temperatures within 1-2°C of the reported values.

*** Hydrodynamic diameters based upon number-averaged intensity measurements via DLS at 37°C and are in agreement with measured diameters from TEM images; average standard deviations of the measurement of multiple particles in TEM are ± 10-15nm.

Although there are a large number of studies on the well-defined assembly of peptides, there have been far fewer studies that exploit intrinsically disordered peptides as a means to generate ordered peptide-based materials; most of the work in related areas has focused on studies of the thermoresponsive elastin-like polypeptides (107-126). Elastin-like (poly)peptides (ELPs), which mimic features of the mammalian protein elastin, are composed largely of Val-Pro-Gly-Xaa-Gly (VPGXG) amino acid repeat units (in which X is any residue except proline). This sequence exhibits the widely exploited lower-critical solution temperature (127-131), in which the ELPs are soluble in water below their transition temperature but will collapse into a coacervate phase above that temperature (132,133). High molecular-weight ELPs have been enormously versatile as smart domains

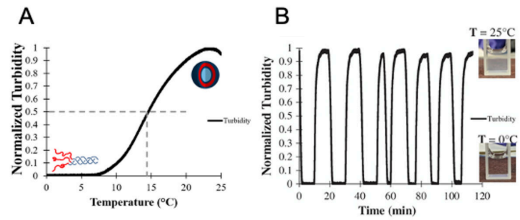

Figure 2. The reversibility of the assembly of dual-thermoresponsive $(VPGFG)_6$-$(GPO)_7$ vesicles (141). (A) Normalized turbidity of $(VPGFG)_6$-$(GPO)_7$vesicles as function of cooling rate as 1 °C/min to define Tt as the temperature at the 50% of maximal turbidity, marked as dashed lines. (B) Normalized turbidity cycling profiles of F6-GPO7 to demonstrate the reversibility of F6-GPO7. Adapted with permission from John Wiley & Sons, Inc., copyright 2020.

in thermally-responsive peptide amphiphilic copolymers and peptide conjugates (134) and have been investigated for manipulating transition temperatures in drug delivery systems and also for targeting cells via thermally-responsive mechanisms (135,136). While these studies illustrate the versatility of the ELPs as self-assembling building blocks, essentially all of the ELPs employed contain tens or even hundreds of pentapeptide repeats. However, short synthetic ELPs, which have high inverse transition temperatures and are thus largely soluble in aqueous solution, have been far more rarely studied (137).

We postulated that the conjugation of CLPs to short ELPs of the general sequence $(VPGXG)_n$-$(GPO)_m$ might offer significant opportunities in the design and assembly of new thermoresponsive nanoparticles, and accordingly, we have synthesized a wide variety of ELP-CLP conjugates in which select ELP and CLP sequences are produced via solid-phase peptide synthesis methods and then conjugated via copper(I)-mediated azide-alkyne cycloaddition (138). The formation of CLP triple helices by the resulting ELP-CLP localizes three short ELP chains at the N-terminal end of the CLP triple helix (Figure 1). The localization of the three ELP chains in this manner enables an LCST-like transition of the ELP domains that is not observed for the corresponding

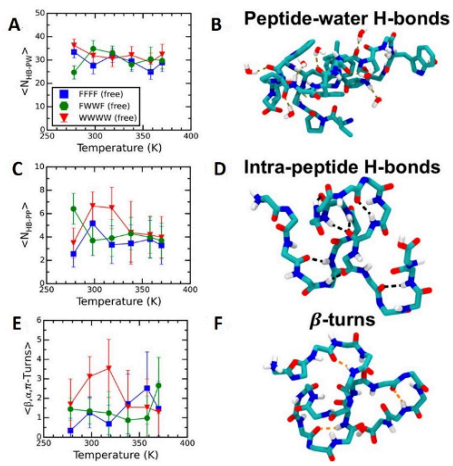

Figure 3. Representative computational results for ELP-CLP conjugates (146). Number of hydrogen bonds between (A) peptide and water and (C) intrapeptide as a function of temperature. (E) β-, α-, and π-turns in peptide as a function of temperature from one free ELP chain atomistic simulations. (B), (D), and (F) are simulation snapshots from one free WWWW system at 318 K representing the parameters plotted in the curves adjacent to the images. For clarity, the hydrogen atoms not contributing to H-bonds with water are not shown in part B; in parts D and F, the side chains are not shown and only hydrogen atoms attached to backbone nitrogen atoms are shown. Adapted with permission from the American Chemical Society, copyright 2019.

ELP peptides alone in solution. Indeed, the resulting ELP-CLP bioconjugates exhibit a remarkably low inverse transition temperature (T_t) after formation of the CLP triple helix (in some cases ca. 80 °C lower than that of the ELP domain alone). This arises from the anchoring and crowding of the ELPs, which reduces the entropic penalty experienced by the ELPs during coacervation at the T_t (139). Well-defined nanostructures can thus be formed under aqueous conditions at temperatures above the T_t of ELP-CLP but only below the melting temperature of the CLP triple helix (T_m); once the CLP triple helix unfolds, the monomeric ELP-CLP conjugate is fully water-soluble (138).

We expected that the dual-phase transitions of the ELP-CLP conjugates could be controlled by details of the amino acid sequences and relative lengths of ELP and CLP blocks that tailor the T_t and T_m, thus stabilizing self-assembled nanostructures at temperatures in between T_t and T_m (85,140-142). The formation of nanostructures that are stable in a narrow range of temperatures between T_t and T_m creates opportunities for designing biocompatible ELP-CLP-based nanomaterials for utilization under biologically relevant conditions. This not only exploits the reversibility of triple helix formation to modulate the transition temperature of the molecules over a wide range but should also permit manipulation of the size and morphologies of the resulting assembled nanostructures. The localization of the collagen domain at the exterior surface of the vesicles also serves as a means to localize nanoparticles in collagen-containing tissues, hydrogels, and films (50,143,144).

Table 2. Transition Temperatures for Select Tyrosine-containing ELP-CLPs

ELP-CLP sequences	T_t
F_6-$(GPO)_8$GG	21.2 ± 2.0°C
F_5Y-$(GPO)_8$GG	20.2 ± 0.9°C
F_4Y_2-$(GPO)_8$GG	16.4 ± 0.4°C
F_3Y_3-$(GPO)_8$GG	12.9 ± 0.2°C
F_5-$(GPO)_8$GG	33.2 ± 0.5°C
F_4Y-$(GPO)_8$GG	34.0 ± 0.4°C
F_3Y_2-$(GPO)_8$GG	31.3 ± 0.3°C
F_2Y_3-$(GPO)_8$GG	28.0 ± 0.5°C

Our studies have indeed shown that the T_t and T_m values of these sequences are easily modulated (Table 1) by varying the composition and length of the $(VPGXG)_n$ ELP domain (both of which serve to modulate the hydrophobicity of the ELP) and perhaps less intuitively also by varying the length and stability of the CLP triple helix (85,140). The use of phenylalanine (F), tyrosine (Y), and tryptophan (W) in the ELP sequences of various lengths, coupled to $(GPO)_n$-based CLP sequences with generally between six and ten repeat units, yield nanostructures with morphologies and dimensions that can be manipulated and thermoresponsiveness that is relevant for

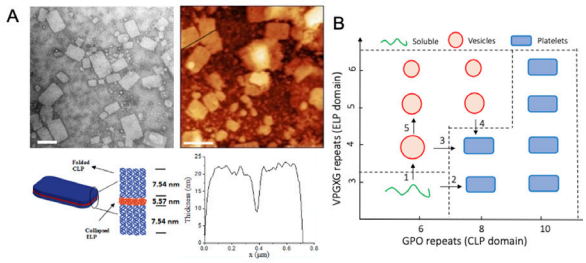

Figure 4. Assembly of ELP-CLP nanoplatelets. (A) TEM and AFM measurements of the FWWF-$(GPO)_8$GG assembly (85). Scale bars = 500 nm. Adapted with permission from the American Chemical Society, copyright 2019. (B) Phase diagram showing morphological transitions possible with appropriate design of ELP-CLP conjugates (142). Adapted with permission from the American Association for the Advancement of Science, copyright 2020.

physiological application and delivery of drugs. Our studies further highlighted the critical influence that the CLP domain also exerts on the ELP-CLP T_t and morphologies of assembled ELP-CLP conjugates, indicating a nuanced relationship between the stability of the CLP and the LCST-like coacervation of the ELP domain (140).

Indeed, a conjugate with the sequence $(VPGFG)_6$-$(GPO)_7$ exhibits highly reversible assembly of well-defined vesicles at a T_t value of ca. 15°C, with a T_m value of ca. 50°C (Figure 2). The dual-temperature responsiveness of the $(VPGFG)_6$-$(GPO)_7$ conjugate further illustrates the feasibility of designing ELP-CLP vesicles that possess both hyperthermic and hypothermic responsiveness, with potential future applications in targeted drug release in the treatment of ECM-related diseases.

A significant advantage of employing peptides in these studies has been the ability to understand molecular-level details that affect the thermal transitions and assembly of the ELP-CLPs via the use of atomistic and coarse-grained (CG) simulations (139,145). Information about chain conformations and structural transitions (e.g., formation of β-turns) as well as hydration (e.g., average number of peptide-water versus peptide-peptide hydrogen bonds) as a function of temperature (Figure 3) has been garnered via an atomistically detailed analysis of ELP and surrounding water molecules. Atomistically-informed CG molecular dynamics simulations have then been applied to evaluate the effect of guest residues on the LCST-like transitions of free ELPs and ELP-CLP conjugates at experimentally relevant concentrations. Even though the net hydrophobicity of an ELP pentad is a key factor that influences the T_t of a given ELP, the molecular origins of the T_t for ELPs containing F, Y, or W are not completely clear, as there are discrepancies in hydrophobicity scales for these amino acid residues (146-150). Computational investigations have thus offered fundamental understanding of the chain-level origins of the ELP phase behavior as well as guidance for the design of thermoresponsive ELP-CLP nanostructures.

For short F-containing ELPs, in their free state and upon conjugation to CLPs, we have observed that the incorporation of the bulkier aromatic residues Y and W induces greater chain stiffness, increased hydrophobic interactions, more facile formation of β-turn structure, and improved π−π overlap, all of which contribute to a lowering in the T_t of an ELP domain with increasing W/Y content (145). These results illustrate reductions in T_t that are completely consistent with the empirical hydrophobicity scales determined for high molecular-weight ELPs and highlight the key design parameters, in addition to hydrophobicity, that can be exploited to tune the LCST-like behavior of these short molecules.

We have demonstrated that Y-containing ELP-CLP conjugates exhibit T_t and T_m transitions that are within physiologically and clinically relevant temperatures for hypo- and hyper-thermic therapies (T_t values shown in Table 2). In addition, the impact of short-range π−π interactions between Y residues enabled finely tuned and reliable manipulation of T_t with the addition of each Y residue, with the position of the Y residues in the ELP-CLP conjugates altering the thermal responsiveness of these conjugates. Observed reductions in T_t were greater with the inclusion of the Y residues at the N-terminal end of the ELP domain; computational results confirm this observation and suggest that locating the Y residues at the N-terminal end permits close enough approach of the Y residues that they can engage in π−π interactions, a possibility that is eliminated when the Y residues are anchored near the CLP and are thus conformationally restricted at distances exceeding that

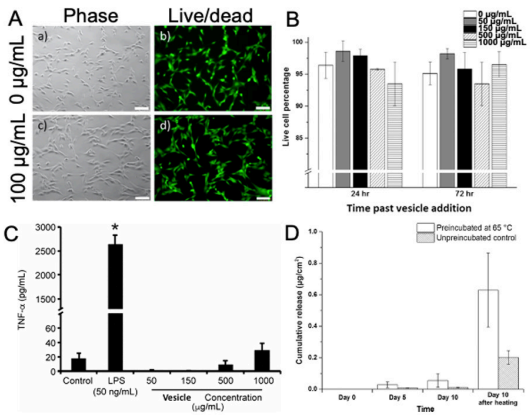

Figure 5. Cytocompatibility and collagen targeting of ELP-CLP vesicles (152). (A) Viability of NIH-3T3 fibroblasts after 24 h incubation with/without ELP-CLP vesicles (100 µg/mL) in serum. Scale bars = 100 µm. (B) Viability of ATDC5 chondrocytes after incubation with ELP-CLP vesicles (0, 50, 100, 500, 1000 µg/mL). (C) Activation of murine-derived RAW264.7 macrophage after 8 h incubation with ELP-CLP vesicles (0, 50, 150, 500, 1000 µg/mL). N = 3; *represents significance from control cultures and cultures treated with vesicles at any concentration ($p < 0.0001$, as determined via ANOVA with Tukey HSD posthoc). (D) Cumulative release of fluorescently labeled ELP-CLP vesicles from type II collagen films as a function of time at room temperature. (N = 4 for a sample preincubated above Tm and N = 3 for the control). Adapted with permission from the American Chemical Society, copyright 2017.

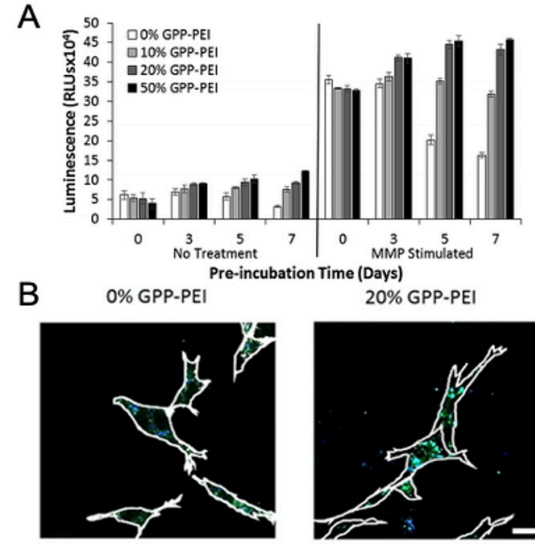

Figure 6. CLP-modified polyplexes in collagen matrix. (A) pGluc expression of sequestered GPP-PEI in the collagen hydrogel and free GPP polyplex in hydrogel with a week pre-incubation in the media with and without metalloproteinase (50). Reproduced with permission from The Royal Society of Chemistry, copyright 2014. (B) Colocalization study of FITC labeled collagen (Green) with Alexa Fluor 350 labeled GPP-PEI (Blue) in fibroblastic cells with five days pre-incubation in the media (49). The scale bar is 25 µm. Reproduced with permission from Elsevier Inc., copyright 2017.

necessary for π−π interactions (Figure 3).

The increase in chain stiffness observed for the more hydrophobic W-containing ELPs suggested that our methods might also be useful for tuning the morphological features of ELP-CLP-based nanostructures. Because of the significant hydrophobicity of W, our original sequences were based on the $(VPGXG)_4$ motif. For sequences with zero or one (VPGWG) pentad, the ELP-CLP conjugates failed to assemble at any temperature, indicating the water solubility of the short ELPs—even those containing W residues. For ELP domains containing two or more (VPGWG) pentads, however, assembly was observed at temperatures greater than 4 °C with an unexpected platelet morphology (Figure 4), which presumably forms because of the relatively rigid nature of the hydrophobic and β-turn forming ELP domains. Tuning the relative lengths of ELP and CLP domains has also proven to be a sensitive parameter for tuning the morphology of these nanostructures, with a threshold ratio of ELP and CLP domain lengths that delineates a transition between spherical vesicles and bilayer platelets (141). The platelets appear to exhibit greater thermo-stability, suggesting mechanisms to tune both stability and morphology of these materials.

These ELP-CLP nanostructures should offer significant opportunities in cargo delivery, and future studies will assess (experimentally and computationally) the impact of cargo encapsulation on assembly. The incorporation of aromatic guest residues in the ELP domain allows adjustment of the T_t and tuning of morphological properties for specific applications and should also facilitate the loading of hydrophobic drugs. The capability of fine-tuning T_t within clinically relevant ranges, either through modification of ELP or CLP domains, will enable designed cargo

delivery profiles. The ability of the ELP-CLP nanostructures to also target collagen-containing matrices should permit their targeting to tissues with aberrant ECM remodeling.

ELP-CLPs for Application in Osteoarthritis

The CLP sequence $(GPO)_4GFOGER(GPO)_4GG$ was employed in the design of initial ELP-CLP conjugates that might be useful for delivery of OA therapeutics (151). CLPs with eight or more GPO repeats exhibit melting temperatures (T_m) above 37 °C and enable formation of stable triple helix at physiological temperature. The peptide sequence GFOGER is widely recognized by several kinds of integrins, such as $\alpha_1\beta_2$, $\alpha_2\beta_1$, and $\alpha_{11}\beta_1$ (152-154), enabling receptor-mediated endocytosis and enhanced gene expression of type II collagen (155,156). An ELP with the sequence $(VPGFG)_6$ would be expected to have a T_t below 37 °C, allowing the conjugate to assemble via collapse of the ELP domain at physiological temperature. Indeed, these conjugates show strong affinity to native collagen through collagen triple helix hybridization and are therefore able to sequester, for at least 21 days, a hydrophobic model compound (fluorescein) in collagen type II films, with subsequent thermally triggered release demonstrating the proof of concept. The vesicles also show high cytocompatibility with both fibroblasts and chondrocytes and essentially no activation of a macrophage cell line (Figure 5). We have also sought to establish that these ELP-CLP nanovesicles could be used to effectively target type II collagen in the joints of mice and have employed a fluorescently labeled ELP-CLP sequence $((VPGFG)_6\text{-}(GPO)_7)$ that was previously shown to have optimal thermal and colloidal stability required for both application and ease of handling (140). We demonstrate (in preparation) that not only do the ELP-CLP vesicles bind to collagen II in films but that they can be retained in the knee joints of mice. These studies highlight the exciting possibility of utilizing ELP-CLP nanovesicles for active targeting of drug therapeutics to the degraded cartilage that is typically found in OA joints.

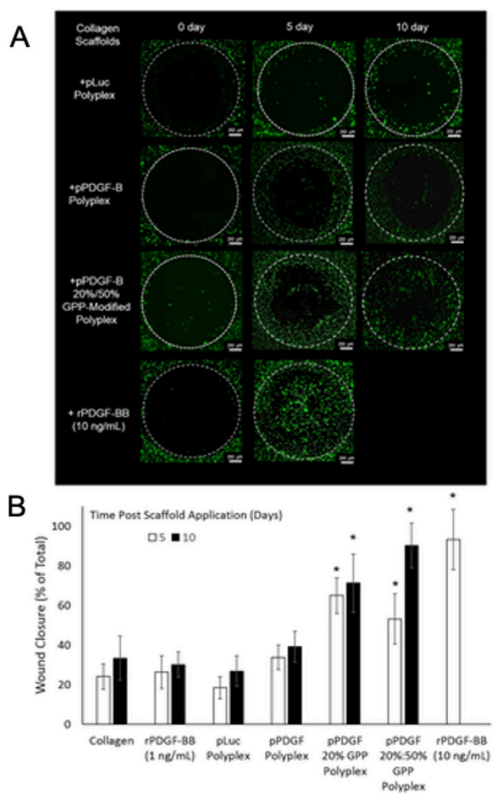

Figure 7. In vitro wound healing assay using CLP-modified polyplex encoding PDGF-BB in collagen matrix (160). (A) Representative images for wound closure by Calcein-AM stained NIH3T3 fibroblasts (Green). (B) The quantification of wound closure using ImageJ. The data represent the mean +/-SD of three separately prepared and analyzed samples. * denotes a statistically-significant difference ($p < .05$) relative to the luciferase-encoding control. Reproduced with permission from John Wiley & Sons, Inc., copyright 2016.

CLP-modified Polyplexes for Wound Healing

The tunable hybridization of CLPs to collagen can also provide improved control of the delivery of other types of nanostructures, such as DNA polyplexes. Collagen-based matrices with encapsulated DNA polyplexes have been utilized to promote improved skin tissue repair or bone regeneration (157,158), and matrices that sequester DNA polyplexes via non-covalent binding demonstrate improvements in transfection efficiencies to fibroblastic cells (71). We have engineered matrices for improved gene transfer by harnessing CLP binding to anchor DNA polyplexes in collagenous tissue, such that cell-mediated collagen remodeling triggers the release and uptake

of the polyplexes as fibroblasts are repairing the tissue. Given that uncoordinated healing is a hallmark in chronic wounds, tailoring of gene delivery profiles via these methods may better match the sequential upregulation of genes observed during normal wound healing processes.

To this end, we have employed PEI-based DNA polyplexes decorated with CLPs (e.g., GPP: $(GPP)_3GPRGEKGERGPR(GPP)_3GPCCG$) to enable sequestration of polyplexes in collagen-containing matrices via triple helix-based binding (49,50,159). Employing cell-mediated collagen turnover as a mechanism for increased gene uptake should have multiple advantages, including improved cell trafficking via engagement of the α2β1 integrin expressed in a wide range of cells (160). In vitro, our CLP-based methods show polyplex retention in collagen I films for up to 35 days (50), with increased and highly robust gene transfer in MMP-stimulated cells (Figure 6A). A collagen-polyplex colocalization study revealed that the CLP-polyplex, along with collagen fragments, were internalized in cells largely via caveolar endocytosis, suggesting integrin interaction with the integrin-binding sites of collagen fragments are involved in cellular internalization (Figure 6B) (49). The benefits of using collagen remodeling as a driver for gene release and activity were confirmed in a more complicated in vivo model, in which transgene expression was localized and extended from three to over 20 days (49).

PDGF represents a particularly appealing target for gene delivery, as it plays a pivotal role in the recruitment of inflammatory cells as well as multiple important processes necessary for healing, including fibroblast proliferation and migration, re-epithelialization, collagen deposition, angiogenesis, and granulation tissue formation within the wound bed (161). Matrix-based strategies for the delivery of PDGF genes exhibit superior healing in experimental chronic wounds (162) although clinical translation has been inhibited by construct escape and limited gene transfer in protein/serum-rich environments (162,163). Improved control over the level, duration, and localization of PDGF gene would greatly

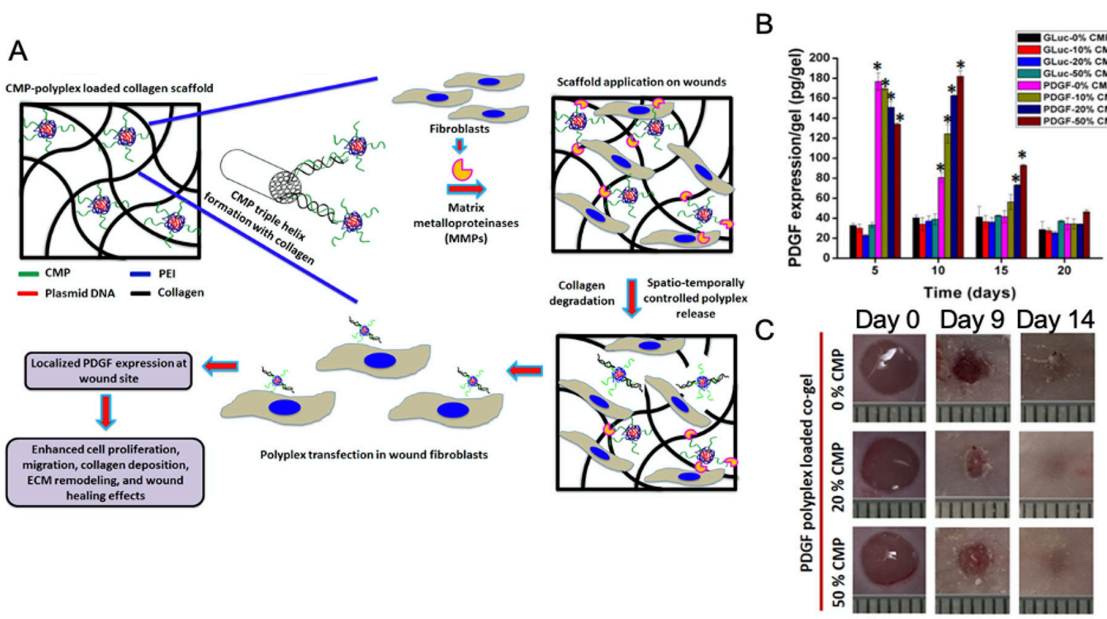

Figure 8. CLP (= CMP) modified PDGF encoding polyplex in co-gel scaffold for wound healing (167). (A) Schematic of the cellular responsive PDGF gene delivery using CLP-modified polyplex loaded co-gel scaffold. (B) TNF-α stimulated In vitro NIH3T3 fibroblasts PDGF expression (or GLuc expression as controls) by CLP modified polyplex loaded co-gel scaffold. (*$P < 0.05$ as compared to GLuc). (C) Images of skin wound closure in mice at Days 0, 9, and 14 after treating with CLP modified PDGF polyplex loaded co-gel. Adapted with permission from the American Chemical Society, copyright 2020.

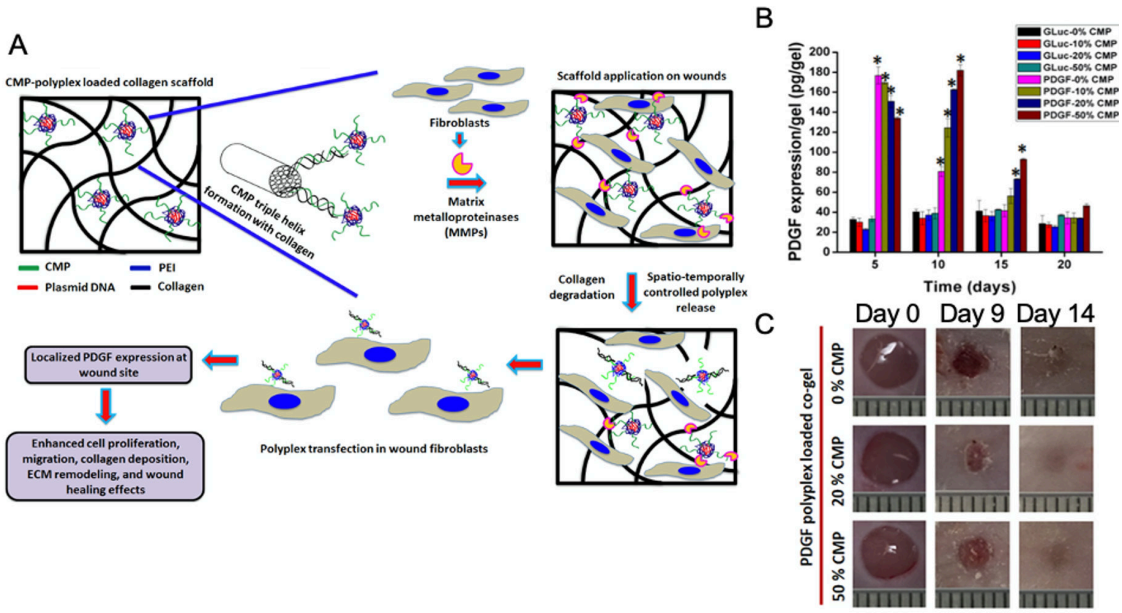

Figure 9. In vivo CLP (= CMP) modified vancomycin liposomes in co-gel scaffold for treatment of MRSA wound infections (169). (A) Schematic of the control of vancomycin release using CLP-modified, vancomycin-loaded liposomes in a co-gel scaffold for anti-bacterial effect. (B) Bacterial counts on mouse punch biopsy wounds inoculated with *Staphylococcus aureus* after treatment with different groups; G1: Punch biopsy wounds + no bacterial inoculation; G2: Punch biopsy wounds + bacterial inoculation; G3: Punch biopsy wounds + bacterial inoculation + blank co-gel; G4: Punch biopsy wounds + bacterial inoculation + Van solution; G5: Punch biopsy wounds + bacterial inoculation + Van loaded co-gel; G5R: Punch biopsy wounds + bacterial inoculation + Van loaded co-gel + re-inoculation at day 1; G6: Punch biopsy wounds + bacterial inoculation + Van-Lipo loaded co-gel; G6R: Punch biopsy wounds + bacterial inoculation + Van-Lipo loaded co-gel + re-inoculation at day 1; G7: Punch biopsy wounds + bacterial inoculation + CMP-Van-Lipo loaded co-gel; G7R: Punch biopsy wounds + bacterial inoculation + CMP-Van-Lipo loaded co-gel + re-inoculation at day 1. (* $P < 0.05$ as compared to G2; † $P < 0.05$ as compared to G3; ‡ $P < 0.05$ as compared to G4; € $P < 0.05$ as compared to G5R; £ $P < 0.05$ as compared to G6; ₡ $P < 0.05$ as compared to G6R). Yellow arrow indicates that the bacterial count couldn't be calculated below 10,000 cfu and hence are indicated as 10,000 cfu for the treatment groups. (n = 3, values represent mean ± standard deviation). H&E staining of G7 for wound healing evaluation and green arrows indicate epidermal thickness. Scale bar is 100 μm. Reproduced with permission from the Elsevier. Inc., copyright 2020.G5: Punch biopsy wounds + bacterial inoculation + Van loaded co-gel; G5R: Punch biopsy wounds + bacterial inoculation + Van loaded co-gel + re-inoculation at day 1; G6: Punch biopsy wounds + bacterial inoculation + Van-Lipo loaded co-gel; G6R: Punch biopsy wounds + bacterial inoculation + Van-Lipo loaded co-gel + re-inoculation at day 1; G7: Punch biopsy wounds + bacterial inoculation + CMP-Van-Lipo loaded co-gel; G7R: Punch biopsy wounds + bacterial inoculation + CMP-Van-Lipo loaded co-gel + re-inoculation at day 1.

advance chronic wound therapies (164,165).

Initial in vitro studies demonstrated that CLP display, on PEI polyplexes encoding PDGF-B, significantly enhanced polyplex activity and PDGF-BB protein expression (ca. four-fold) even after exposure to serum for seven days at 37 °C (49). Collagen remodeling and cell migration were also enhanced by CLPs, as highlighted through collagen contraction assays and cell migration studies. The promising capacity for the CLP-polyplex/collagen gels in wound scaffold applications was demonstrated by increased cell densities and accelerated migration of fibroblasts (NIH 3T3) in collagen-based in vitro 3D wound models (Figure 7). Defects treated with CLP-modified collagens reached approximately 90% wound closure after 10 days of treatment, whereas wound closure never exceeded 40% using scaffolds containing unmodified polyplex. The use of gene transfer was significantly more effective than protein-based delivery; in fact, rPDGF-BB levels had to be increased

by an order of magnitude to achieve similar bioactivity as that observed in CLP-modified scaffolds. The increase in gene stability and improved expression associated with CLP-based gene delivery may translate in vivo, aiding in multiple aspects of wound repair.

To test this, we aimed to develop a biomaterial scaffold able to recruit fibroblast cells in vivo and harness cell-mediated collagen-turnover to trigger PDGF gene delivery and thereby stimulate enhanced skin wound healing (166). We prepared a robust collagen-fibrin containing, provisional-like matrix with CLPs (CLP/PDGF gene-modified 'co-gels,' Figure 8) to capture aspects of the natural healing environment (167) and to enable facile application within the wound bed. CLP-polyplex-modified co-gel scaffolds permitted highly tunable, sustained release of polyplexes for up to 24 days, with release and expression profiles that could be tailored depending upon the amount of CLP incorporated in the polyplexes. As we had observed for CLP-polyplex-modified collagen-only scaffolds, release was dependent upon matrix metalloproteinase (MMP)-mediated remodeling of the collagen scaffold, in this case with ~30% higher PDGF expression by MMP-producing fibroblasts in vitro as compared with non-MMP producing cells.

The integration of fibrin with the gene-modified collagens resulted in co-gels that strongly supported both fibroblast cell recruitment/invasion as well as multiple aspects of the longer-term healing response. In vivo wound healing studies established faster wound closure (~80% wound closure in nine days) with minimal scar formation following the application of CLP-modified PDGF gene-incorporating collagen scaffolds and with improved collagen production, cell proliferation, cell migration, and myofibroblast activity in vivo (Figure 8).

These strategies also enable delivery of therapeutics that treat multiple aspects of the chronic wound environment, including infection. CLPs were conjugated to the surface of vancomycin-loaded liposomes via maleimide-thiol click chemistry, and CLP-tethered liposomal particles (CMP-Van-Lipo) were incorporated into the collagen-fibrin scaffolds for sustained liposome retention and Van delivery (168). Tethering CMP-Van-Lipo to co-gels sustained Van delivery in vitro, as compared to Van-Lipo or Van-Lipo loaded co-gels, for up to 48 hours. These antibacterial effects of CMP-Van-Lipo loaded co-gels were successfully translated in vivo in an MRSA-inoculated murine excisional wound model (Figure 9) and were retained even following a second fresh bacterial inoculation on the wound. This study is a proof-of-concept for the potential application of CMP-Van-Lipo loaded co-gels for sustained antimicrobial release and potential infection control in wounds.

Taken together, our findings stress the advantages of CLP-mediated GF gene therapies for enabling effective wound healing in vivo and providing substantial reductions in GF exposure, which may reduce concerns with both cost and safety. The methods are also valuable, with appropriately modified carriers, for extending the duration of release of small-molecule therapeutics. These advantages highlight the potential of CLP-triggered gene delivery to enhance numerous collagen-based materials through improved non-viral gene delivery regimens. Future studies involving chronic wound models (with existing co-morbidities such as diabetes and bacterial colonization in wound site) are thus warranted to further confirm the applicability of co-gels for chronic wound healing.

CONCLUSIONS

We have demonstrated that CLP conjugation can be used to tune ELP T_t transitions and morphological features of ELP-CLP conjugates, which in the future should enable finely tuned, thermally triggered release of cargo by hypo- and hyperthermic treatments. The computational modeling of the molecular transitions will enable significant opportunities to design carriers for specific applications. The delivery of macromolecular cargo (e.g., DNA) has also been improved via CLP-based approaches, enabling cell-mediated delivery of functional genes from collagen-containing matrices, with demonstrated efficacy in the treatment of wounds in vivo. Our ability to make these advances has been enabled by a collaborative approach that has merged molecular-level materials design with the predictive capabilities of computation. The applications development has been possible only with collaboration with groups with expertise in specific cell signaling and human pathologies.

Many opportunities and challenges remain in further development of these CLP-based strategies. For example, the delivery of multiple drugs from a single matrix-based carrier will require judicious selection of peptide components and an understanding of how the binding of drugs affects the thermoresponsivesness and morphologies of ELP-CLP conjugates. On-demand drug release with a high level of specificity for a select cell type will require modification of the CLP domain and/or the nanocarrier surface. The use of multiple ECM-inspired peptides may also offer a promising strategy to increase affinity to a particular cell type, using information about the cell's natural ECM receptor expression patterns, or to promote the sequential delivery of a series of drugs.

ACKNOWLEDGMENTS

The authors are grateful for the financial support that has enabled these contributions. Various aspects of the work described have been funded by the National Science Foundation (BMAT, BME, CBET, and PFI programs) and the National Institutes of Health (NIDCD, SIG, and COBRE programs). None of this work would have been possible without the hard work and dedication of the many students who have been advised and co-advised in the laboratories of the collaborators. Special thanks are owed to Jeongmin Hwang for compiling of references and figures for this manuscript. We also thank Ohm Krishna, Tianzhi Luo, Michael David, Rebecca Scott, Morgan Urello, Raj Thapa, Lucas Dunshee, Jingya Qin, Haofu Huang, Joshua Condon, Ammu Prhashanna, Phillip Taylor, Ryan McDonough, Colleen Fridley, Jeongmin Hwang, and Anuraag Boddupalli for their contributions to this work and offer thanks to our colleagues and core facilities staff across the UD campus.

REFERENCES

1. Huang G, Huang H. Hyaluronic acid-based biopharmaceutical delivery and tumor-targeted drug delivery system. J Control Release. 2018;278:122-126.
2. Fu S, Xu X, Ma Y, Zhang S, Zhang S. RGD peptide-based non-viral gene delivery vectors targeting integrin alphavbeta3 for cancer therapy. J Drug Target. 2019;27(1):1-11.
3. Nikam RR, Gore KR. Journey of siRNA: clinical developments and targeted delivery. Nucleic Acid Ther. 2018;28(4):209-224.
4. Goodman SL, Picard M. Integrins as therapeutic targets. Trends Pharmacol Sci. 2012;33(7):405-12.
5. Raab-Westphal S, Marshall JF, Goodman SL. Integrins as therapeutic targets: successes and cancers. Cancers (Basel). 2017;9(9).
6. Ramshaw JA, Peng YY, Glattauer V, Werkmeister JA. Collagens as biomaterials. J Mater Sci Mater Med. 2009;20 Suppl 1:S3-8.
7. Hinderer S, Layland SL, Schenke-Layland K. ECM and ECM-like materials - biomaterials for applications in regenerative medicine and cancer therapy. Adv Drug Deliv Rev. 2016;97:260-9.
8. Benton G, Arnaoutova I, George J, Kleinman HK, Koblinski J. Matrigel: from discovery and ECM mimicry to assays and models for cancer research. Adv Drug Deliv Rev. 2014;79-80:3-18.
9. Sawkins MJ, Saldin LT, Badylak SF, White LJ. Extracellular matrix for tissue engineering and biomaterials. In: Berardi AC, editor. ECM hydrogels for regenerative medicine, stem cell biology and regenerative medicine. Charm (Switzerland): Human Press; 2018. p 27-58.
10. Jacob J, Haponiuk JT, Thomas S, Gopi S. Biopolymer based nanomaterials in drug delivery systems: a review. Mater Today Chem. 2018;9:43-55.
11. Chia CL, Shelat VG, Low W, George S, Rao J. The use of Collatamp G, local gentamicin-collagen sponge, in reducing wound infection. Int Surg. 2014;99(5):565-70.
12. Lozeau LD, Grosha J, Kole D, Prifti F, Dominko T, Camesano TA, Rolle MW. Collagen tethering of synthetic human antimicrobial peptides cathelicidin LL37 and its effects on antimicrobial activity and cytotoxicity. Acta Biomater. 2017;52:9-20.
13. Ishihara J, Ishihara A, Sasaki K, Lee SS, Williford JM, Yasui M, Abe H, Potin L, Hosseinchi P, Fukunaga K and others. Targeted antibody and cytokine cancer immunotherapies through collagen affinity. Sci Transl Med. 2019;11(487).
14. Zitnay JL, Li Y, Qin Z, San BH, Depalle B, Reese SP, Buehler MJ, Yu SM, Weiss JA. Molecular level detection and localization of mechanical damage in collagen enabled by collagen hybridizing

peptides. Nat Commun. 2017;8(1):14913.
15. Hwang J, Huang Y, Burwell TJ, Peterson NC, Connor J, Weiss SJ, Yu SM, Li Y. In situ imaging of tissue remodeling with collagen hybridizing peptides. ACS Nano. 2017;11(10):9825-9835.
16. Luo J, Tong YW. Self-assembly of collagen-mimetic peptide amphiphiles into biofunctional nanofiber. ACS Nano. 2011;5(10):7739-7747.
17. Luo T, Kiick KL. Collagen-like peptide bioconjugates. Bioconjugate Chem. 2017;28(3):816-827.
18. Xing R, Liu K, Jiao T, Zhang N, Ma K, Zhang R, Zou Q, Ma G, Yan X. An injectable self-assembling collagen–gold hybrid hydrogel for combinatorial antitumor photothermal/photodynamic therapy. Adv Mater. 2016;28(19):3669-3676.
19. Johnson VL, Hunter DJ. The epidemiology of osteoarthritis. Best Pract Res Clin Rheumatol. 2014;28(1):5-15.
20. Mandl LA. Osteoarthritis year in review 2018: clinical. Osteoarthr Cartil. 2019;27(3):359-364.
21. Hawker GA. Osteoarthritis is a serious disease. Clin Exp Rheumatol. 2019;37(5):3-6.
22. Hunter DJ, Neogi T, Hochberg MC. Quality of osteoarthritis management and the need for reform in the US. Arthritis Care Res. 2011;63(1):31-38.
23. Blanco FJ, Guitian R, Vazquez-Martul E, de Toro FJ, Galdo F. Osteoarthritis chondrocytes die by apoptosis - a possible pathway for osteoarthritis pathology. Arthritis Rheum. 1998;41(2):284-289.
24. Goldring MB, Goldring SR. Articular cartilage and subchondral bone in the pathogenesis of osteoarthritis. Ann N Y Acad Sci. 2010;1192:230-237.
25. Lowman EW. Osteoarthritis. JAMA. 1955;157(6):487-488.
26. Maldonado M, Nam J. The role of changes in extracellular matrix of cartilage in the presence of inflammation on the pathology of osteoarthritis. Biomed Res Int. 2013:10.
27. Goldring SR, Goldring MB. Clinical aspects, pathology and pathophysiology of osteoarthritis. J Musculoskel Neuron. 2006;6(4):376-378.
28. Glyn-Jones S, Palmer AJR, Agricola R, Price AJ, Vincent TL, Weinans H, Carr AJ. Osteoarthritis. Lancet. 2015;386(9991):376-387.
29. Immonen J, Siefring C. Age- and occupation-based public health considerations related to osteoarthritis of the knee joint: a cadaveric study. Cartilage. 2019;10(2):238-244.
30. Evans CH, Kraus VB, Setton LA. Progress in intra-articular therapy. Nat Rev Rheumatol. 2014;10(1):11-22.
31. Grodzinsky AJ, Wang Y, Kakar S, Vrahas MS, Evans CH. Intra-articular dexamethasone to inhibit the development of post-traumatic osteoarthritis. J Orthop Res. 2017;35(3):406-411.
32. Evans CH, Kraus VB, Setton LA. Progress in intra-articular therapy. Nat Rev Rheumatol. 2014;10(1):11-22.
33. Geiger BC, Grodzinsky AJ, Hammond PT. Designing drug delivery systems for articular joints. Chem Eng Prog. 2018;114(5):46-51.
34. Larsen C, Ostergaard J, Larsen SW, Jensen H, Jacobsen S, Lindegaard C, Andersen PH. Intra-articular depot formulation principles: role in the management of postoperative pain and arthritic disorders. J Pharm Sci. 2008;97(11):4622-4654.
35. Guidolin D. Intra-articular 500-730 kDa hyaluronan (Hyalgan((R))) therapy in the management of osteoarthritis. Can a specific therapeutic profile be defined? Eur Rev Med Pharmacol Sci. 2018;22(14):4698-4719.
36. Printz JO, Lee JJ, Knesek M, Urquhart AG. Conflict of interest in the assessment of hyaluronic acid injections for osteoarthritis of the knee: an updated systematic review. J Arthroplasty. 2013;28(8):30-+.
37. Oo WM, Liu X, Hunter DJ. Pharmacodynamics, efficacy, safety and administration of intra-articular therapies for knee osteoarthritis. Expert Opin Drug Metab Toxicol. 2019.
38. Xing D, Wang B, Zhang W, Yang Z, Hou Y, Chen Y, Lin J. Intra-articular hyaluronic acid injection in treating knee osteoarthritis: assessing risk of bias in systematic reviews with ROBIS tool. Int J Rheum Dis. 2017;20(11):1658-1673.
39. Wehling P, Evans C, Wehling J, Maixner W. Effectiveness of intra-articular therapies in osteoarthritis: a literature review. Ther Adv Musculoskelet Dis. 2017;9(8):183-196.
40. Johansen M, Bahrt H, Altman RD, Bartels EM, Juhl CB, Bliddal H, Lund H, Christensen R. Exploring reasons for the observed inconsistent

trial reports on intra-articular injections with hyaluronic acid in the treatment of osteoarthritis: meta-regression analyses of randomized trials. Semin Arthritis Rheu. 2016;46(1):34-48.
41. Nguyen C, Lefevre-Colau M-M, Poiraudeau S, Rannou F. Evidence and recommendations for use of intra-articular injections for knee osteoarthritis. Ann Phys Rehabil Med. 2016;59(3):184-189.
42. Rosen J, Avram V, Fierlinger A, Niazi F, Sancheti P, Bedi A. Clinicians' perspectives on the use of intra-articular hyaluronic acid as a treatment for knee osteoarthritis: a North American, multidisciplinary survey. Clin Med Insights Arthritis Musculoskelet Disord. 2016;9:21-27.
43. Bajpayee AG, Quadir MA, Hammond PT, Grodzinsky AJ. Charge based intra-cartilage delivery of single dose dexamethasone using avidin nano-carriers suppresses cytokine-induced catabolism long term. Osteoarthr Cartil. 2016;24(1):71-81.
44. Bajpayee AG, Scheu M, Grodzinsky AJ, Porter RM. Electrostatic interactions enable rapid penetration, enhanced uptake and retention of intra-articular injected avidin in rat knee joints. J Orthop Res. 2014;32(8):1044-1051.
45. Bajpayee AG, Grodzinsky AJ. Cartilage-targeting drug delivery: can electrostatic interactions help? Nat Rev Rheumatol. 2017;13(3):183-193.
46. Wang AY, Mo X, Chen CS, Yu SM. Facile modification of collagen directed by collagen mimetic peptides. J Am Chem Soc. 2005;127(12):4130-4131.
47. Chattopadhyay S, Guthrie KM, Teixeira L, Murphy CJ, Dubielzig RR, McAnulty JF, Raines RT. Anchoring a cytoactive factor in a wound bed promotes healing. J Tissue Eng Regen Med. 2016;10(12):1012-1020.
48. Lin AH, Zitnay JL, Li Y, Yu SM, Weiss JA. Microplate assay for denatured collagen using collagen hybridizing peptides. J Orthop Res. 2019;37(2):431-438.
49. Urello MA, Kiick KL, Sullivan MO. ECM turnover-stimulated gene delivery through collagen-mimetic peptide-plasmid integration in collagen. Acta Biomater. 2017;62:167-178.
50. Urello MA, Kiick KL, Sullivan MO. A CMP-based method for tunable, cell-mediated gene delivery from collagen scaffolds. J Mat Chem B. 2014;2(46):8174-8185.
51. Li Y, Yu SM. Targeting and mimicking collagens via triple helical peptide assembly. Curr Opin Chem Biol. 2013;17(6):968-975.
52. Singh A, Corvelli M, Unterman SA, Wepasnick KA, McDonnell P, Elisseeff JH. Enhanced lubrication on tissue and biomaterial surfaces through peptide-mediated binding of hyaluronic acid. Nat Mater. 2014;13(10):988-95.
53. Nussbaum SR, Carter MJ, Fife CE, DaVanzo J, Haught R, Nusgart M, Cartwright D. An economic evaluation of the impact, cost, and medicare policy implications of chronic nonhealing wounds. Value Health. 2018;21(1):27-32.
54. Bennett NT, Schultz GS. Growth factors and wound healing: Part II. Role in normal and chronic wound healing. Am J Surg. 1993;166(1):74-81.
55. Macri L, Clark RAF. Tissue engineering for cutaneous wounds: selecting the proper time and space for growth factors, cells and the extracellular matrix. Skin Pharmacol Phys. 2009;22(2):83-93.
56. Rees RS, Robson MC, Smiell JM, Perry BH, Pressure Ulcer Study G. Becaplermin gel in the treatment of pressure ulcers: a phase II randomized, double-blind, placebo-controlled study. Wound Repair Regen. 1999;7(3):141-147.
57. Margolis DJ, Crombleholme T, Herlyn M. Clinical protocol: phase I trial to evaluate the safety of H5.020CMV.PDGF-B for the treatment of a diabetic insensate foot ulcer. Wound Repair Regen. 2000;8(6):480-493.
58. Zhang S, Uludağ H. Nanoparticulate systems for growth factor delivery. Pharm Res. 2009;26(7):1561.
59. Robson MC, Mustoe TA, Hunt TK. The future of recombinant growth factors in wound healing. Am J Surg. 1998;176(2, Supplement 1):80S-82S.
60. Mitchell AC, Briquez PS, Hubbell JA, Cochran JR. Engineering growth factors for regenerative medicine applications. Acta Biomater. 2016;30:1-12.
61. Shahryari A, Saghaeian Jazi M, Mohammadi S, Razavi Nikoo H, Nazari Z, Hosseini ES,

Burtscher I, Mowla SJ, Lickert H. Development and clinical translation of approved gene therapy products for genetic disorders. Front Genet. 2019;10:868.
62. Shepard JA, Wesson PJ, Wang CE, Stevans AC, Holland SJ, Shikanov A, Grzybowski BA, Shea LD. Gene therapy vectors with enhanced transfection based on hydrogels modified with affinity peptides. Biomaterials. 2011;32(22):5092-5099.
63. Lei Y, Huang S, Sharif-Kashani P, Chen Y, Kavehpour P, Segura T. Incorporation of active DNA/cationic polymer polyplexes into hydrogel scaffolds. Biomaterials. 2011;31(34):9106-9116.
64. Turner NJ, Badylak SF. The use of biologic scaffolds in the treatment of chronic nonhealing wounds. Adv Wound Care. 2015;4(8):490-500.
65. Tyrone JW, Mogford JE, Chandler LA, Ma CL, Xia YP, Pierce GF, Mustoe TA. Collagen-embedded platelet-derived growth factor DNA plasmid promotes wound healing in a dermal ulcer model. J Surg Res. 2000;93(2):230-236.
66. Segura T, Shea LD. Surface-tethered DNA complexes for enhanced gene delivery. Bioconjugate Chem. 2002;13(3):621-629.
67. Wang C, Ma L, Gao C. Design of gene-activated matrix for the repair of skin and cartilage. Polym J. 2014;46(8):476-482.
68. Segura T, Volk MJ, Shea LD. Substrate-mediated DNA delivery: role of the cationic polymer structure and extent of modification. J Control Release. 2003;93(1):69-84.
69. Elangovan S, D'Mello SR, Hong L, Ross RD, Allamargot C, Dawson DV, Stanford CM, Johnson GK, Sumner DR, Salem AK. The enhancement of bone regeneration by gene activated matrix encoding for platelet derived growth factor. Biomaterials. 2014;35(2):737-747.
70. Wang C-HK, Pun SH. Substrate-mediated nucleic acid delivery from self-assembled monolayers. Trends Biotechnol. 2011;29(3):119-126.
71. Orsi S, De Capua A, Guarnieri D, Marasco D, Netti PA. Cell recruitment and transfection in gene activated collagen matrix. Biomaterials. 2010;31(3):570-576.
72. Rosler A, Vandermeulen GW, Klok HA. Advanced drug delivery devices via self-assembly of amphiphilic block copolymers. Adv Drug Deliv Rev. 2001;53(1):95-108.
73. Zhao X, Pan F, Xu H, Yaseen M, Shan H, Hauser CA, Zhang S, Lu JR. Molecular self-assembly and applications of designer peptide amphiphiles. Chem Soc Rev. 2010;39(9):3480-98.
74. Ariga K, Nishikawa M, Mori T, Takeya J, Shrestha LK, Hill JP. Self-assembly as a key player for materials nanoarchitectonics. Sci Technol Adv Mater. 2019;20(1):51-95.
75. Acar H, Srivastava S, Chung EJ, Schnorenberg MR, Barrett JC, LaBelle JL, Tirrell M. Self-assembling peptide-based building blocks in medical applications. Adv Drug Deliv Rev. 2017;110:65-79.
76. Dimatteo R, Darling NJ, Segura T. In situ forming injectable hydrogels for drug delivery and wound repair. Adv Drug Deliv Rev. 2018;127:167-184.
77. Spicer CD, Jumeaux C, Gupta B, Stevens MM. Peptide and protein nanoparticle conjugates: versatile platforms for biomedical applications. Chem Soc Rev. 2018;47(10):3574-3620.
78. Stewart MP, Langer R, Jensen KF. Intracellular delivery by membrane disruption: mechanisms, strategies, and concepts. Chem Rev. 2018;118(16):7409-7531.
79. Zou QL, Liu K, Abbas M, Yan XH. Peptide-modulated self-assembly of chromophores toward biomimetic light-harvesting nanoarchitectonics. Adv Mater. 2016;28(6):1031-1043.
80. Thomas F, Burgess NC, Thomson AR, Woolfson DN. Controlling the assembly of coiled-coil peptide nanotubes. Angew Chem Int Ed. 2016;55(3):987-991.
81. Wu DD, Sinha N, Lee J, Sutherland BP, Halaszynski NI, Tian Y, Caplan J, Zhang HV, Saven JG, Kloxin CJ and others. Polymers with controlled assembly and rigidity made with click-functional peptide bundles. Nature. 2019;574(7780):658-+.
82. Beesley JL, Woolfson DN. The de novo design of alpha-helical peptides for supramolecular self-assembly. Curr Opin Biotech. 2019;58:175-182.
83. Sato K, Ji W, Palmer LC, Weber B, Barz M, Stupp SI. Programmable assembly of peptide amphiphile via noncovalent-to-covalent bond conversion. J Am Chem Soc. 2017;139(26):8995-9000.
84. Sarkar B, O'Leary LER, Hartgerink JD.

Self-assembly of fiber-forming collagen mimetic peptides controlled by triple-helical nucleation. J Am Chem Soc. 2014;136(41):14417-14424.
85. Qin J, Luo T, Kiick KL. Self-assembly of stable nanoscale platelets from designed elastin-like peptide-collagen-like peptide bioconjugates. Biomacromolecules. 2019;20(4):1514-1521.
86. Bachinger HP, Engel J. The thermodynamics and kinetics of collagen folding. Protein Folding Handbook. 2005:1059-1110.
87. Brodsky B, Persikov AV. Molecular structure of the collagen triple helix. Adv Protein Chem. 2005;70:301-339.
88. Fallas JA, Dong JH, Tao YZJ, Hartgerink JD. Structural insights into charge pair interactions in triple helical collagen-like proteins. J Biol Chem. 2012;287(11):8039-8047.
89. Persikov AV, Ramshaw JAM, Brodsky B. Prediction of collagen stability from amino acid sequence. J Biol Chem. 2005;280(19):19343-19349.
90. He LR, Theato P. Collagen and collagen mimetic peptide conjugates in polymer science. Eur Polym J. 2013;49(10):2986-2997.
91. Strauss K, Chmielewski J. Advances in the design and higher-order assembly of collagen mimetic peptides for regenerative medicine. Curr Opin Biotechnol. 2017;46:34-41.
92. Acevedo-Jake AM, Ngo DH, Hartgerink JD. Control of collagen triple helix stability by phosphorylation. Biomacromolecules. 2017;18(4):1157-1161.
93. Jiang T, Meyer TA, Modlin C, Zuo X, Conticello VP, Ke Y. Structurally ordered nanowire formation from co-assembly of DNA origami and collagen-mimetic peptides. J Am Chem Soc. 2017;139(40):14025-14028.
94. Przybyla DE, Chmielewski J. Metal-triggered radial self-assembly of collagen peptide fibers. J Am Chem Soc. 2008;130(38):12610-12611.
95. Persikov AV, Ramshaw JAM, Kirkpatrick A, Brodsky B. Amino acid propensities for the collagen triple-helix. Biochemistry. 2000;39(48):14960-14967.
96. O'Leary LER, Fallas JA, Bakota EL, Kang MK, Hartgerink JD. Multi-hierarchical self-assembly of a collagen mimetic peptide from triple helix to nanofibre and hydrogel. Nat Chem. 2011;3(10):821-828.
97. Bretscher LE, Jenkins CL, Taylor KM, DeRider ML, Raines RT. Conformational stability of collagen relies on a stereoelectronic effect. J Am Chem Soc. 2001;123(4):777-778.
98. Rele S, Song YH, Apkarian RP, Qu Z, Conticello VP, Chaikof EL. D-periodic collagen-mimetic microfibers. J Am Chem Soc. 2007;129(47):14780-14787.
99. Krishna OD, Kiick KL. Supramolecular assembly of electrostatically stabilized, hydroxyproline-lacking collagen-mimetic peptides. Biomacromolecules. 2009;10(9):2626-2631.
100. Tanrikulu IC, Forticaux A, Jin S, Raines RT. Peptide tessellation yields micrometre-scale collagen triple helices. Nat Chem. 2016;8:1008.
101. Zitnay JL, Li Y, Qin Z, San BH, Depalle B, Reese SP, Buehler MJ, Yu SM, Weiss JA. Molecular level detection and localization of mechanical damage in collagen enabled by collagen hybridizing peptides. Nat Commun. 2017;8(1):14913.
102. Nelson CM, Bissell MJ. Of extracellular matrix, scaffolds, and signaling: tissue architecture regulates development, homeostasis, and cancer. Annu Rev Cell Dev Biol. 2006;22(1):287-309.
103. Sargeant TD, Desai AP, Banerjee S, Agawu A, Stopek JB. An in situ forming collagen–PEG hydrogel for tissue regeneration. Acta Biomater. 2012;8(1):124-132.
104. Krishna OD, Wiss KT, Luo T, Pochan DJ, Theato P, Kiick KL. Morphological transformations in a dually thermoresponsive coil–rod–coil bioconjugate. Soft Matter. 2012;8(14):3832-3840.
105. Luo TZ, He LR, Theato P, Kiick KL. Thermoresponsive self-assembly of nanostructures from a collagen-like peptide-containing diblock copolymer. Macromol Biosci. 2015;15(1):111-123.
106. Luo TZ, Kiick KL. Collagen-like peptides and peptide-polymer conjugates in the design of assembled materials. Eur Polym J. 2013;49(10):2998-3009.
107. Li NK, Roberts S, Quiroz FG, Chilkoti A, Yingling YG. Sequence directionality dramatically affects LCST behavior of elastin-like polypeptides. Biomacromolecules. 2018;19(7):2496-2505.
108. McDaniel JR, Radford DC, Chilkoti A. A

unified model for De Novo design of elastin-like polypeptides with tunable inverse transition temperatures. Biomacromolecules. 2013;14(8):2866-2872.
109. Tarakanova A, Buehler MJ, Huang W, Kaplan D. Exploiting elastin's mutability: Regulated design of elastin-like and silk-elastin-like protein polymer libraries in simulation and experiment. Tissue Eng Part A. 2015;21:S26-S26.
110. Li NK, Quiroz FG, Hall CK, Chilkoti A, Yingling YG. Molecular description of the LCST behavior of an elastin-like polypeptide. Biomacromolecules. 2014;15(10):3522-3530.
111. Heinz A, Schrader CU, Baud S, Keeley FW, Mithieux SM, Weiss AS, Neubert RHH, Schmelzer CEH. Molecular-level characterization of elastin-like constructs and human aortic elastin. Matrix Biol. 2014;38:12-21.
112. Golas EI, Czaplewski C. Rapid communication computational simulation and analysis of a candidate for the design of a novel silk-based biopolymer. Biopolymers. 2014;101(9):915-923.
113. Tarakanova A, Buehler MJ. Molecular modeling of protein materials: case study of elastin. Model Simul Mat Sci Eng. 2013;21(6).
114. Seo M, Rauscher S, Pomes R, Tieleman DP. Improving internal peptide dynamics in the coarse-grained MARTINI model: toward large-scale simulations of amyloid- and elastin-like peptides. J Chem Theory Comput. 2012;8(5):1774-1785.
115. Rauscher S, Pomes R. Aggregated yet disordered: a molecular simulation study of the self-aggregation of elastin. Biophys J. 2012;102(3):40A-40A.
116. Arkin H, Bilsel M. How conformational transition depends on hydrophobicity of elastin-like polypeptides. Eur Phys J E. 2010;31(3):327-332.
117. Vogel M. Temperature-dependent mechanisms for the dynamics of protein-hydration waters: a molecular dynamics simulation study. J Phys Chem B. 2009;113(28):9386-9392.
118. Nuhn H, Klok H-A. Secondary structure formation and LCST behavior of short elastin-like peptides. Biomacromolecules. 2008;9(10):2755-2763.
119. Glaves R, Baer M, Schreiner E, Stoll R, Marx D. Conformational dynamics of minimal elastin-like polypeptides: the role of proline revealed by molecular dynamics and nuclear magnetic resonance. Chemphyschem. 2008;9(18):2759-2765.
120. Krukau A, Brovchenko I, Geiger A. Temperature-induced conformational transition of a model elastin-like peptide GVG(VPGVG)(3) in water. Biomacromolecules. 2007;8(7):2196-2202.
121. Baer M, Schreiner E, Kohlmeyer A, Rousseau R, Marx D. Inverse temperature transition of a biomimetic elastin model: reactive flux analysis of folding/unfolding and its coupling to solvent dielectric relaxation. J Phys Chem B. 2006;110(8):3576-3587.
122. Floquet N, Hery-Huynh S, Dauchez M, Derreumaux P, Tamburro AM, Alix AJP. Structural characterization of VGVAPG, an elastin-derived peptide. Biopolymers. 2004;76(3):266-280.
123. Arkin H. Searching low-energy conformations of two elastin sequences. Eur Phys J B. 2004;37(2):223-228.
124. Li B, Daggett V. Molecular basis for the extensibility of elastin. J Muscle Res Cell M. 2002;23(5-6):561-573.
125. Li B, Alonso DOV, Daggett V. The molecular basis for the inverse temperature transition of elastin. J Mol Biol. 2001;305(3):581-592.
126. Li B, Alonso DOV, Bennion BJ, Daggett V. Hydrophobic hydration is an important source of elasticity in elastin-based biopolymers. J Am Chem Soc. 2001;123(48):11991-11998.
127. Nettles DL, Chilkoti A, Setton LA. Applications of elastin-like polypeptides in tissue engineering. Adv Drug Deliv Rev. 2010;62(15):1479-1485.
128. Betre H, Ong SR, Guilak F, Chilkoti A, Fermor B, Setton LA. Chondrocytic differentiation of human adipose-derived adult stem cells in elastin-like polypeptide. Biomaterials. 2006;27(1):91-99.
129. Panitch A, Yamaoka T, Fournier MJ, Mason TL, Tirrell DA. Design and biosynthesis of elastin-like artificial extracellular matrix proteins containing periodically spaced fibronectin CS5 domains. Macromolecules. 1999;32(5):1701-1703.
130. Wright ER, McMillan RA, Cooper A, Apkarian RP, Conticello VP. Thermoplastic elastomer hydrogels via self-assembly of an elastin-mimetic

triblock polypeptide. Adv Funct Mater. 2002;12(2):149-154.
131. Daamen WF, Veerkamp JH, van Hest JCM, van Kuppevelt TH. Elastin as a biomaterial for tissue engineering. Biomaterials. 2007;28(30):4378-4398.
132. Raphel J, Parisi-Amon A, Heilshorn SC. Photoreactive elastin-like proteins for use as versatile bioactive materials and surface coatings. J Mater Chem. 2012;22(37):19429-19437.
133. Huang L, McMillan RA, Apkarian RP, Pourdeyhimi B, Conticello VP, Chaikof EL. Generation of synthetic elastin-mimetic small diameter fibers and fiber networks. Macromolecules. 2000;33(8):2989-2997.
134. Meyer DE, Chilkoti A. Quantification of the effects of chain length and concentration on the thermal behavior of elastin-like polypeptides. Biomacromolecules. 2004;5(3):846-851.
135. Callahan DJ, Liu W, Li X, Dreher MR, Hassouneh W, Kim M, Marszalek P, Chilkoti A. Triple stimulus-responsive polypeptide nanoparticles that enhance intratumoral spatial distribution. Nano Lett. 2012;12(4):2165-2170.
136. Trabbic-Carlson K, Setton LA, Chilkoti A. Swelling and mechanical behaviors of chemically cross-linked hydrogels of elastin-like polypeptides. Biomacromolecules. 2003;4(3):572-580.
137. Hassan M, Martin AD, Thordarson P. Engineering biocompatible scaffolds through the design of elastin-based short peptides. ChemPlusChem. 2018;83(1):47-52.
138. Luo T, Kiick KL. Noncovalent modulation of the inverse temperature transition and self-assembly of elastin-b-collagen-like peptide bioconjugates. J Am Chem Soc. 2015;137(49):15362-5.
139. Condon JE, Jayaraman A. Development of a coarse-grained model of collagen-like peptide (CLP) for studies of CLP triple helix melting. J Phys Chem B. 2018;122(6):1929-1939.
140. Dunshee LC, Sullivan MO, Kiick KL. Manipulation of the dually thermoresponsive behavior of peptide-based vesicles through modification of collagen-like peptide domains. Bioeng Transl Med. 2020;5(1).
141. Qin J, Sloppy JD, Kiick KL. Fine structural tuning of the assembly of ECM peptide conjugates via slight sequence modifications. Sci Adv. 2020;6(41).
142. Taylor PA, Huang H, Kiick KL, Jayaraman A. Placement of tyrosine residues as a design element for tuning the phase transition of elastin-peptide-containing conjugates: experiments and simulations. Molecular Systems Design & Engineering. 2020;5(7):1239-1254.
143. Mo X, An YJ, Yun CS, Yu SM. Nanoparticle-assisted visualization of binding interactions between collagen mimetic peptide and collagen fibers. Angew Chem Int Ed. 2006;45(14):2267-2270.
144. Li Y, Foss CA, Summerfield DD, Doyle JJ, Torok CM, Dietz HC, Pomper MG, Yu SM. Targeting collagen strands by photo-triggered triple-helix hybridization. Proc Natl Acad Sci U S A. 2012;109(37):14767-14772.
145. Prhashanna A, Taylor PA, Qin J, Kiick KL, Jayaraman A. Effect of peptide sequence on the LCST-like transition of elastin-like peptides and elastin-like peptide-collagen-like peptide conjugates: simulations and experiments. Biomacromolecules. 2019;20(3):1178-1189.
146. Hopp TP, Woods KR. Prediction of protein antigenic determinants from amino acid sequences. Proc Natl Acad Sci U S A. 1981;78(6):3824-3828.
147. Kyte J, Doolittle RF. A simple method for displaying the hydropathic character of a protein. J Mol Biol. 1982;157(1):105-132.
148. Von Heijne G. Membrane protein structure prediction: hydrophobicity analysis and the positive-inside rule. J Mol Biol. 1992;225(2):487-494.
149. Monera OD, Sereda TJ, Zhou NE, Kay CM, Hodges RS. Relationship of sidechain hydrophobicity and α-helical propensity on the stability of the single-stranded amphipathic α-helix. J Pept Sci. 1995;1(5):319-329.
150. Boyd D, Schierle C, Beckwith J. How many membrane proteins are there? Protein Sci. 1998;7(1):201-205.
151. Luo T, David MA, Dunshee LC, Scott RA, Urello MA, Price C, Kiick KL. Thermoresponsive elastin-b-collagen-like peptide bioconjugate nanovesicles for targeted drug delivery to collagen-containing matrices. Biomacromolecules. 2017;18(8):2539-2551.

152. Knight CG, Morton LF, Peachey AR, Tuckwell DS, Farndale RW, Barnes MJ. The collagen-binding A-domains of integrins alpha(1)beta(1) and alpha(2)beta(1) recognize the same specific amino acid sequence, GFOGER, in native (triple-helical) collagens. J Biol Chem. 2000;275(1):35-40.
153. Zhang WM, Kapyla J, Puranen JS, Knight CG, Tiger CF, Pentikainen OT, Johnson MS, Farndale RW, Heino J, Gullberg D. alpha(11) beta(1) integrin recognizes the GFOGER sequence in interstitial collagens. J Biol Chem. 2003;278(9):7270-7277.
154. Reyes CD, Garcia AJ. Engineering integrin-specific surfaces with a triple-helical collagen-mimetic peptide. J Biomed Mater Res A. 2003;65A(4):511-523.
155. Mhanna R, Ozturk E, Vallmajo-Martin Q, Millan C, Muller M, Zenobi-Wong M. GFOGER-modified MMP-sensitive polyethylene glycol hydrogels induce chondrogenic differentiation of human mesenchymal stem cells. Tissue Eng Part A. 2014;20(7-8):1165-1174.
156. Zeltz C, Orgel J, Gullberg D. Molecular composition and function of integrin-based collagen glues-introducing COLINBRIs. Biochim Biophys Acta. 2014;1840(8):2533-48.
157. Guo R, Xu S, Ma L, Huang A, Gao C. Enhanced angiogenesis of gene-activated dermal equivalent for treatment of full thickness incisional wounds in a porcine model. Biomaterials. 2010;31(28):7308-20.
158. Elangovan S, D'Mello SR, Hong L, Ross RD, Allamargot C, Dawson DV, Stanford CM, Johnson GK, Sumner DR, Salem AK. The enhancement of bone regeneration by gene activated matrix encoding for platelet derived growth factor. Biomaterials. 2014;35(2):737-47.
159. Urello MA, Kiick KL, Sullivan MO. Integration of growth factor gene delivery with collagen-triggered wound repair cascades using collagen-mimetic peptides. Bioeng Transl Med. 2016;1(2):207-219.
160. Arosio D, Casagrande C. Advancement in integrin facilitated drug delivery. Adv Drug Deliv Rev. 2016;97:111-43.
161. McGary EC, Weber K, Mills L, Doucet M, Lewis V, Lev DC, Fidler IJ, Bar-Eli M. Inhibition of platelet-derived growth factor-mediated proliferation of osteosarcoma cells by the novel tyrosine kinase inhibitor STI571. Clin Cancer Res. 2002;8(11):3584.
162. Gu D-l, Nguyen T, Gonzalez AM, Sonsnowski BA, Phillips ML, Chandler LA. Adenovirus encoding human platelet-derived growth factor delivered in collagen exhibits safety, biodistribution, and immunogenicity profiles favorable for clinical use. Mol Ther. 2004;9(5):699-711.
163. Blume P, Driver VR, Tallis AJ, Kirsner RS, Kroeker R, Payne WG, Wali S, Marston W, Dove C, Engler RL and others. Formulated collagen gel accelerates healing rate immediately after application in patients with diabetic neuropathic foot ulcers. Wound Repair Regen. 2011;19(3):302-308.
164. Schleef M, Blaesen M, Schmeer M, Baier R, Marie C, Dickson G, Scherman D. Production of non viral DNA vectors. Curr Gene Ther. 2010;10(6):487-507.
165. Elsabahy M, Nazarali A, Foldvari M. Non-viral nucleic acid delivery: key challenges and future directions. Curr Drug Deliv. 2011;8(3):235-244.
166. Thapa RK, Margolis DJ, Kiick KL, Sullivan MO. Enhanced wound healing via collagen-turnover-driven transfer of PDGF-BB gene in a murine wound model. ACS Appl Bio Mater. 2020.
167. Shepherd J, Bax D, Best S, Cameron R. Collagen-fibrinogen lyophilised scaffolds for soft tissue regeneration. Materials. 2017;10(6):568.
168. Thapa RK, Kiick KL, Sullivan MO. Encapsulation of collagen mimetic peptide-tethered vancomycin liposomes in collagen-based scaffolds for infection control in wounds. Acta Biomater. 2020;103:115-128.